Cloud species classification from video recordings

D P Egorov[1], B G Kutuza[1], A B Akvilonova[2] and O V Kravchenko[1,3]

[1] Kotel'nikov Institute of Radio Engineering and Electronics of RAS, Mokhovaya st. 11-7, Moscow, 125009, Russian Federation
[2] Fryazino Branch of Kotel'nikov Institute of Radio Engineering and Electronics of RAS, Vvedensky Ave., 1, Fryazino, 141190, Russian Federation
[3] Federal Research Center "Computer Science and Control" of RAS, Vavilova st., 40, Moscow, 119333, Russian Federation

E-mail: e-mail@dobrix.ru

Abstract. Large data bank of images has been accumulated during atmospheric cloudiness ground-based observations from 2017 to 2020 near Fryazino city, Moscow Region. The problem of obtained images classification into several types is considered. The types are clear sky (no clouds); cumulus cloudiness of various extent (humilis, mediocris, congestus); very powerful clouds such as cumulonimbus or nimbostratus; stratus cloud cover; stratocumulus clouds; light and high-positioned clouds (altocumulus, cirrus, cirrostratus and cirrocumulus). A qualitative analysis of the key features of gray, blue, green and red level co-occurrence matrices for various pixel distances and directions (angles) is performed to solve the problem. An image classification algorithm based on these and other key features retrieved during image preprocessing is developed. The quality evaluation is performed. The developed software tool is currently successfully used for atmospheric radiometry problems support.

1. Introduction

The influence of various weather conditions on the downwelling atmospheric K-band radiation fluctuations is considered by the authors in [1]. The data obtained during the experiment on brightness temperature spectral measurements, which have been performed in Fryazino branch of Kotel'nikov Institute of Radioengeneering and Electronics of RAS since 2017, are analyzed. Continuous measurements have been conducted by ground-based multi-frequency radiometer-spectrometer with improved fluctuation sensitivity and great gain coefficient temperature stability [2]. Simultaneously, the two meteostations located nearby registered near-surface thermodynamic temperature, absolute humidity of air and atmospheric pressure. The duration of measurement sessions vary from 2 to 5 hours. During this time, weather conditions can change significantly. However, the authors considered only those measurement sessions during which the quality of cloud cover stays strictly the same – either clear sky or cumulus clouds of certain vertical extent is observed. Measurement sessions with mixed cloudiness were not allowed. Selection of measurement sessions by this criteria was performed manually by viewing and doing markup of synchronized middle-quality video recordings (figure 1). Video camera was set at the same zenith angle as the radiometer antenna.

Figure 1. Still from the video dated August 14, 2018, 14:04 UTC+3. Cumulus humilis.

Accumulated experimental data of microwave radiometry with their subsequent categorization by cloud cover type (clear sky, cumulus fractus/humilis/mediocris/congestus, cumulonimbus) allowed to clarify the nature of fluctuations in downwelling radiation near the line 22.235 GHz of resonant absorption of water vapor. Spectra of brightness temperature structural function [3] for wide range of spatial-temporal intervals are obtained. The value of square root of structural function performes here as measure of radiation fluctuation intensity. Linear regression of fluctuation intensity versus near-surface air temperature and absolute humidity under clear sky conditions was considered. The evaluation of liquid water content of observed cloudiness was held by means of dual-frequency radiometric method of integral moisture content retrieval. The dependence of brightness temperature fluctuation intensity on session-averaged value of liquid water content was obtained. To clarify all aforesaid dependencies and continue to systematically research the effect of various meteorological factors and other cloud species including non-convective ones on atmospheric radiation fluctuations there is a compelling need for development an algorithm for comprehensive automatic classification of video recordings by types of cloudiness observed.

2. Approaches

One of the most actual problem related to the Earth remote sensing data processing is recognition of clouds of certain species or other objects on satellite images. To solve this problem, methods of texture analysis are widely used. There are various approaches to measuring and description of the image texture – statistical, geometric, structural (or syntactic), spectral [4, 5]. Among the statistical methods, the gray-level co-occurrence histogram evaluation method [6] is widely known and proven itself well. The gray-level co-occurrence histogram $P = P(i, j, d, \theta)$ is a 4D-array the values of which represent the number of times that gray-level j occurs at a distance d and at an angle θ from gray-level i. Assume there are L possible gray or brightness levels in total (usually $L = 256$), then P is $L \times L$ in shape for fixed d and θ.

$$P_{d,\theta}(i,j) = \left|\{(k,l)\,,\ (\xi,\eta):\ I\,(k,l) = i,\ I\,(\xi,\eta) = j\}\right|, \tag{1}$$

where i and j are quantized brightness levels, $I(k, l)$ and $I(\xi, \eta)$ are the values of brightness at pixels with corresponding coordinates, d is distance between these pixels and θ is horizontal angle or direction.

After the co-occurrence histogram P is obtained from original image converted to a grayscale, the following summary features [7] each computed for fixed distance d and angle θ can be

considered:

$$\text{“contrast”:}\quad f_1 = \sum_{i,j=0}^{L-1} (i-j)^2 \cdot P_{d,\theta}(i,j). \tag{2}$$

$$\text{“dissimilarity”:}\quad f_2 = \sum_{i,j=0}^{L-1} |i-j| \cdot P_{d,\theta}(i,j). \tag{3}$$

$$\text{“homogeneity”:}\quad f_3 = \sum_{i,j=0}^{L-1} \frac{P_{d,\theta}(i,j)}{1+(i-j)^2}. \tag{4}$$

$$\text{“energy”:}\quad f_4 = \sqrt{\sum_{i,j=0}^{L-1} P_{d,\theta}^2(i,j)}. \tag{5}$$

$$\text{“correlation”:}\quad f_5 = \sum_{i,j=0}^{L-1} \frac{(i-\bar{i})(j-\bar{j})}{\sqrt{\sigma_i^2 \sigma_j^2}} P_{d,\theta}(i,j), \tag{6}$$

where $\bar{i}$, $\bar{j}$ are mean levels and σ_i, σ_j are standard deviations.

We use these texture features for the analysis. Note that the co-occurrence histogram P can be calculated not only for grayscale converted image, but also for blue, green and red channel of the image separately. In some cases, this can provide some additional information, but unlikely.

Another approach that should be classified as a statistical one was implemented by the authors and consists in filtering the original image transformed to HSV color space with a set of threshold filters, followed by extraction of contours [8] and calculation of various characteristics related. The lower and upper thresholds for S and V color components are chosen empirically, are constant and the same for all filters. The lower threshold l_* for H component is also constant, but the upper one $l^*, l^* > l_*$ changes from filter to filter with some predetermined step. Of course, there can be many variations here. However, with a change in the upper threshold, a transition to another filter occurs, which leads to new results of the algorithm for contour extraction. On every filter change new set of contours is obtained (figure 2). Only external contours with an area larger than the size of the smallest of the considered clouds in pixels are under interest (other contours are to be eliminated).

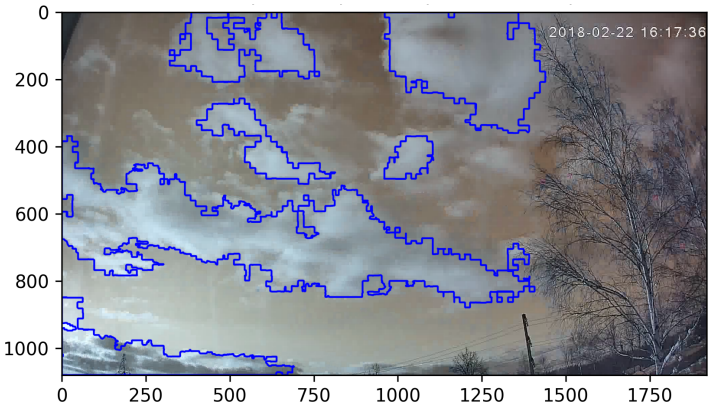

Figure 2. Still from the video dated February 22, 2018, 16:17 UTC+3, with contours extracted.

Finding all pixels of original image belonging to any of the contours extracted, features of minimum, maximum, mean and variance of brightness or certain color can be introduced. Similar statistics for contour areas can be considered. These features were also used for the analysis.

3. Data processing

Initially, 120 images per each cloud cover category under consideration have been manually marked up. A training set of 960 images has been formed. One example of the training dataset is a vector of 2911 features which includes 2160 features obtained by gray, blue, green and red level co-occurrence histograms postprocessing (5 features for 27 various pixel distances and 4 angles times 4 channels), 735 features obtained by threshold filtering and contour extraction method (with 21 features for 35 filters) and the remaining 16 features – minimum, maximum, mean and variance values for 3 colors of the whole original image and one channel of grayscale image. The distances for co-occurrence histograms are 1, 2, ..., 9, 10, 20, ... 90, 100, 150, ..., 450, 500. The angles are 0°, 45°, 90° and 135°. To compute the specified features in a reasonable time, the multiprocessing (CPU-bound) technology has been involved. All features f_i^j, $0 \le i < 2911$, $0 \le j < 960$ have been additionally scaled as $\widetilde{f}_i^j = \left(f_i^j - \overline{f_i}\right)/\sigma_i$, where $\overline{f_i}$ is the mean and σ_i is the standard deviation of the training samples.

Such a set of characteristics is undoubtedly highly redundant. For example, $P_{d,\theta}$ histogram is always very similar to $P_{(d\pm1),\theta}$ that is why the features retrieved for the first and the second case will be highly correlated. To reduce the feature space, two methods have been used. The first is RFE (Recursive Feature Elimination [9]) with random forest classifier as the core. This method consists in fitting the given machine learning algorithm, ranking features by importance, discarding the least important features, and further re-fitting the model. The process is repeated iteratively until a specified number of features remains. In figure 3 a t-SNE (t-distributed Stochastic Neighbor Embedding, visualization method [10]) 2D-representation of the 20 features remained after RFE algorithm application is shown. At each iteration of RFE only one feature is being removed from the initial scaled feature space. T-SNE perplexity is 30, maximum number of iterations for the optimization is 1000.

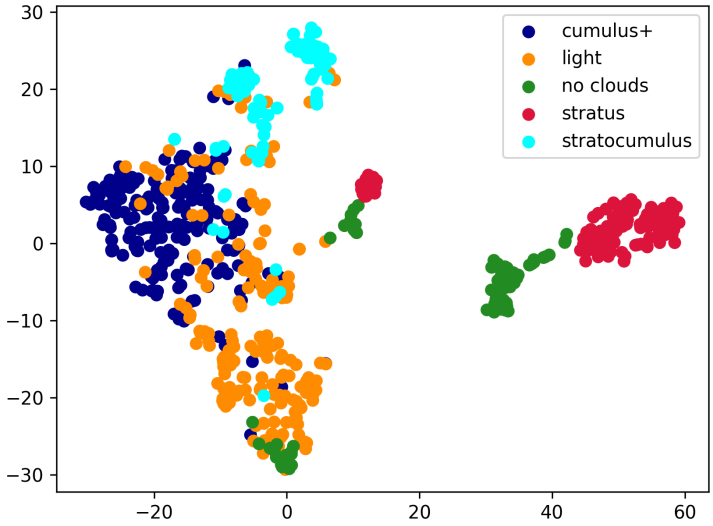

Figure 3. T-SNE representation of 20 features selected by RFE algorithm (with random forest classifier, 100 estimators). Blue – cumulus humilis to congestus, cumulonimbus and nimbostratus (3 initial subcategories are combined, 360 images); orange – cumulus fractus, cirrocumulus and cirrostratus cloud species (2 initial subcategories are combined, 240 images); green – no clouds observed (120 images); red – stratus cloud cover (120 images); cyan – stratocumulus clouds (120 images).

The second algorithm for selection of significant features also uses a classifier to estimate their importance. The n-th iteration is to choose a random feature, fit the given classifier with

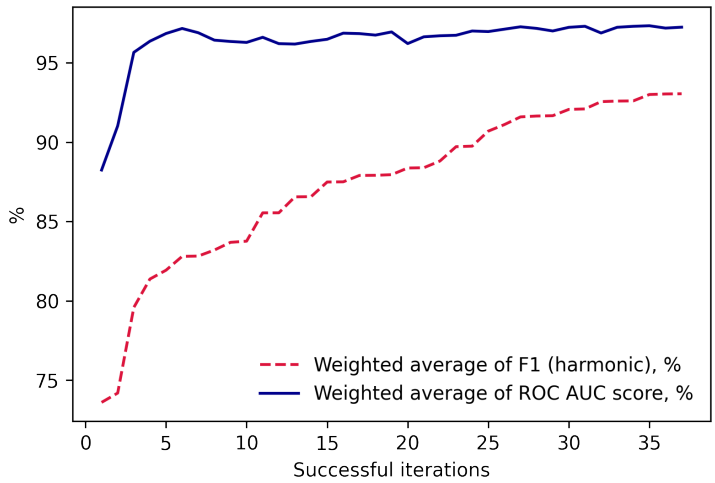

Figure 4. The dependencies of test data classification scores on successful iteration number: accuracy, F1 and roc-auc in percentages (2nd method).

subset of already selected features updated with the current one. If the accuracy or F1-score of classifier predictions on test data using newest combination of features is greater (than using the previous combination), then the current feature is to be added to the subset of selected features. After new feature is added, check operations are performed. If ignoring of any earlier selected feature in the formed subset does not lead to decrease in classification accuracy or F1-score, then this feature is to be eliminated. Let us call the iteration which adds or eliminates one feature "successful". In figure 4 the dependencies of test data classification F1-score and roc-auc score (percentages) on successful iterations are shown. The problem of classification into 5 categories is solved here (see figure 3). Test data make up one third of the entire randomized dataset (training data make up two thirds). Random forest classifier with 100 estimators is used. F1-score is average weighted by class support (the number of true instances for each class). Roc-auc score is also weighted in such way and averaged, at that AUC of each class is calculated against the rest [11]. Exactly average weighted F1-metric is used as key indicator for feature importance here, but not accuracy metric due to imbalance in number of examples for each class. In 36 successful iterations, 22 parameters out of 2911 were selected.

4. Conclusion

The problem of images classification into several types of cloud cover has been considered. The texture features retrieval statistical method of gray-level co-occurrence histogram evaluation has been implemented. An approach based on threshold filtering the images, followed by extraction of contours and further related statistics calculation has been described. Small training dataset has been created with the features computed in parallel. Two algorithms for insignificant feature elimination has been used. The RFE algorithm with random forest classifier has been applied and the corresponding t-SNE 2D-representation of remained features has been presented. By means of the second algorithm, it has been managed to fit the model up to average weighted F1-score 0.93 with average weighted roc-auc score 0.96 (obtained on test data) while solving five categories classification problem (random forest classifier with 100 estimators used). Based on the results obtained, a software tool for automatic classification of images by cloud types and video markup has been developed. Further work will be aimed at improving the quality of classification.

References

[1] Egorov D P and Kutuza B G 2020 Atmospheric Brightness Temperature Fluctuations in the Resonance Absorption Band of Water Vapor 18-27.2 GHz *IEEE Trans. Geosci. Remote Sens.* Early Access pp 1-8

[2] Egorov D P and Kutuza B G 2020 The Influence of Clouds on Atmospheric Radiation Fluctuations in the Resonance Absorption Band of Water Vapor 18-27.2 GHz *Journal of Physics: Conference Series* 1632 (2020) 012010

[3] Kutuza B G 2003 Spatial and Temporal Fluctuations of the Atmospheric Microwave Emission *Radio Sci.* vol 38 no 3 pp 12-1–12-7

[4] Fralenko V P 2014 Methods of Image Texture Analysis, Earth Remote Sensing Data Processing *Program Systems: Theory and Applications* no 4(22) pp 19-39

[5] Astafurov V G and Skorokhodov A V 2015 Multi-layer Cloud Classification from MODIS Data using Neural Network Technology and Fuzzy Logic Approach *Sovremennye problemy distantsionnogo zondirovaniya Zemli iz kosmosa* vol 12 no 6 pp 162-173

[6] Haralick R M 1979 Statistical and Structural Approaches to Texture *Proceedings of the IEEE* vol 67 no 5 pp 768-804

[7] Hall-Beyer, Mryka 2017 *GLCM Texture: A Tutorial v. 3.0* (University of Calgary's Digital Repository) 76 p

[8] Bradski G, Kaehler A 2008 *Learning OpenCV: Computer vision with the OpenCV library* (O'Reilly Media)

[9] Jason Brownlee 2020 *Recursive Feature Elimination (RFE) for Feature Selection in Python* Online: https://machinelearningmastery.com/rfe-feature-selection-in-python/

[10] Laurens van der Maaten and Geoffrey Hinton 2008 Visualizing Data using t-SNE *Journal of Machine Learning Research* vol 9 pp 2579-2605

[11] Fawcett T 2006 An introduction to ROC analysis *Pattern Recognition Letters* vol 27(8) pp 861-874